I&EC research
Industrial & Engineering Chemistry Research

pubs.acs.org/IECR

Article

Study on Controlled Synthesis of Mesoporous Pseudoboehmite via Carbonation Reaction

Chengqian Zhang, Youzhi Liu,* Yuliang Li, Shuwei Guo, Shufei Wang, Shangyuan Cheng, and Hongyan Shen

Cite This: https://doi.org/10.1021/acs.iecr.3c04662

Read Online

ACCESS | Metrics & More | Article Recommendations

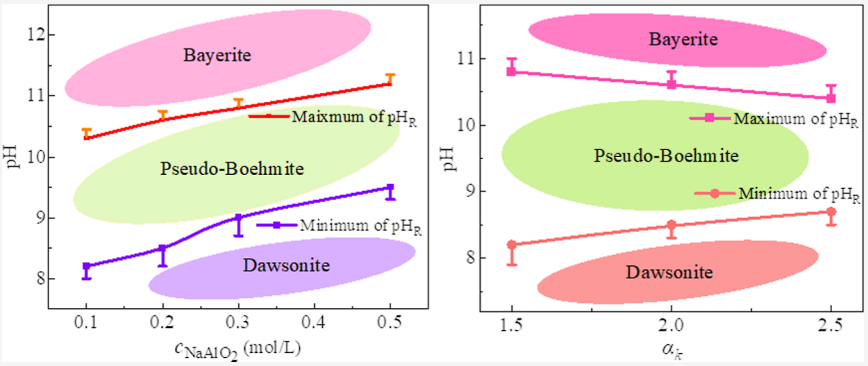

ABSTRACT: Pseudoboehmite is a precursor for mesoporous-activated alumina and is widely employed in catalysis and adsorption applications. The carbonation reaction is recognized as the most environmentally friendly and cost-effective production method. However, its susceptibility to impurity formation poses challenges in practical applications. The control of the reaction end point pH is crucial for ensuring purity. Currently, there is a lack of research on the influence of sodium aluminate solution concentration and composition ratio (α_k) on the reaction end point pH and its impact on the crystallization mechanism. This research extensively explored the effects of the sodium aluminate solution concentration and α_k on the carbonation process. Analysis of crystalline phases under different conditions emphasized the critical influence of concentration and α_k on the critical end point pH of pseudoboehmite synthesis and its impact on the crystallization mechanism. The results revealed significant effects of the concentration and α_k on the pH change during the carbonation reaction. Increasing concentration raised both the maximum and minimum end point pH values, while elevated α_k had the opposite effect. Increasing α_k and concentration led to a narrowing of the pH range at the end point of the carbonation reaction for preparing pseudoboehmite. The study revealed that pseudoboehmite and Bayerite crystals were generated from two different sodium aluminate decomposition pathways, which challenges the conventional understanding of the crystalline growth mechanism of aluminum hydroxide. Reducing the pH value of the reaction end point accelerated the nucleation of pseudoboehmite and inhibition of Bayerite. Ultimately, successfully synthesizing mesoporous pseudoboehmite and activated alumina, with a pore volume of 0.44 cm^3/L, surface area of 242.76 m^2/g, and average pore diameter of 7.3 nm, this study not only supported precise reaction control and enhanced production efficiency but also offered insights for eco-friendly utilization of CO_2, thus contributing to a more sustainable and environmentally friendly production process.

1. INTRODUCTION

Pseudoboehmite (PB), as the precursor of mesoporous activated alumina, is widely used as a catalyst or catalyst support and binder in various processes, such as petroleum refining,[1] alcohol dehydration,[2] methanol steam reforming,[3] and Fischer−Tropsch process[4] due to its inexpensiveness, high mechanical strength, and tunable pore size. The methods for preparing pseudoboehmite include neutralization,[5−13] alcohol aluminum,[14−16] and carbonation reaction methods.[17−25] Carbonation reaction of $NaAlO_2$ solution with CO_2 gas has become one of the most economical techniques for the commercial preparation of PB because the $NaAlO_2$ solution is an intermediate product of the production process of alumina by bauxite, and the operating cost of flue gas containing carbon dioxide is low.[21,25−27] The sodium carbonate wastewater generated by the carbonation reaction can be recycled by

Received: January 3, 2024
Revised: February 15, 2024
Accepted: March 11, 2024

smelting bauxite. Thus, research on the preparation of aluminum hydroxide by carbonation reaction has not stopped for nearly 3 decades.

The sodium aluminate solution is mainly derived from the Bayer process or the alkaline process of smelting bauxite. Additionally, with the increasing demands for environmental protection and the development of resource recycling, businesses not only smelt bauxite but also are now utilizing aluminum-rich fly ash,[26,28−30] coal gangue,[31] red mud,[31,32] waste alumina,[17,33,34] and nuclear-contaminated sludge[13,35,36] to extract aluminum to produce sodium aluminate solution. Due to variations in raw materials and processing techniques, the concentration and component ratios of sodium aluminate solution differ, thereby influencing the process and reaction conditions of carbonate reaction to produce pseudoboehmite, consequently affecting process control and the properties of the products. Currently, there are no reported studies on the influence of sodium aluminate solution concentration and component ratios on the conditions of carbonate reaction for preparation of pseudoboehmite. Therefore, studying the impact of different sodium aluminate solutions on the carbonation reaction for the preparation of pseudoboehmite is of great significance for academic research and industrial production.

The sodium aluminate solution contains free sodium hydroxide (NaOH), sodium aluminate ($NaAl(OH)_4$), and other trace substances. The presence of free sodium hydroxide in the sodium aluminate solution is essential for maintaining solution stability.[37,38] The term α_k is defined as the ratio of the amount-of-substance concentration between sodium hydroxide and aluminum hydroxide in sodium aluminate solution, representing the content of sodium hydroxide in the sodium aluminate solution. The concentrations of sodium hydroxide and sodium aluminate influence the changes in pH in the liquid phase of the carbonate reaction. Although pH variation curves of sodium aluminate solution during the carbonate reaction have been reported multiple times,[21,39,40] the complete recording of the entire process has been lacking. The impacts of different sodium aluminate solution components and concentrations on the carbonate reaction process have not been investigated.

The carbonation reaction of sodium aluminate solution can be described by the following equations

$$CO_2(g) \rightarrow CO_2(aq) \quad (1)$$

$$NaOH + CO_2 \rightarrow NaHCO_3 \quad (2)$$

$$NaHCO_3 + NaOH \rightarrow Na_2CO_3 \quad (3)$$

$$NaAl(OH)_4 \xrightarrow{k_3} Al(OH)_3 + NaOH \quad (4)$$

Carbon dioxide gas enters the liquid phase. At the same time, it reacts with sodium hydroxide to form sodium bicarbonate and sodium carbonate, as shown in eq 2 and 3. As the pH of the solution decreases, sodium aluminate decomposes to form aluminum hydroxide solid, as shown in eq 4.

Some studies have reported the influence of α_k on the formation of bayerite (B) and gibbsite (G) in the carbonation reaction. However, there is currently no relevant literature on the impact of α_k on the end point pH of the reaction in preparing pseudoboehmite through the carbonate reaction. Jiang et al.[20] and Xiaobin et al.[41] found that sodium hydroxide promotes the growth of gibbsite and trihydrate aluminum hydroxide crystals. Marinos et al.[21,42] discovered that high concentrations of sodium carbonate are conducive to the formation of sodalite aluminum hydroxide, and temperatures above 65 °C favor the direct precipitation of sodalite aluminum hydroxide.

Several papers[26,39,43,44] suggest that the end point pH of the carbonation reaction is a key determinant of the crystalline phase of aluminum hydroxide generated in the carbonation reaction. Lu et al.'s study[26] indicates that a sodium aluminate solution containing 40 g/L alumina produces pseudoboehmite at carbonation reaction end point pH values of 11 and 10.5, gibbsite at pH 11.5, and sodalite aluminum hydroxide at pH 9.5. Yang et al.[36] reported the formation of pseudoboehmite at neutralization reaction end point pH < 10. The study by Ren et al.[43] highlighted the preparation of pseudoboehmite using 0.05 and 0.1 mol/L sodium aluminate solutions at carbonation reaction end point pH values of 9.5 and 10.5, respectively. Wang et al.[44] found that 10.5 was the maximum value of end point pH for the preparation of pseudoboehmite through the carbonation reaction using a 0.2 mol/L sodium aluminate solution. Yang et al.[45] indicates the formation of pseudoboehmite at the carbonation reaction end point pH = 10.5 and the generation of Dawsonite(DA) at pH = 8.5, without specifying the concentration of sodium aluminate solution. The reported end point pH of the carbonation reaction for preparing pseudoboehmite is different, and the maximum and minimum values of the reaction end point pH have not been systematically reported. Further, there are no relevant reports on the influence of sodium aluminate solution concentration and α_k on the reaction end point pH for preparing pseudoboehmite through the carbonation reaction. Although the research on the preparation of pseudoboehmite through the carbonation reaction has continued for 2 decades, it is still a challenge to explain the mechanism by which the end point pH of the carbonation reaction determines the crystalline phase.

Therefore, this study first thoroughly investigates the impact of the sodium aluminate solution concentration and α_k on pH changes during the carbonation reaction. Subsequently, through a detailed analysis of aluminum hydroxide crystalline phases, the study explores the carbonation reaction end point pH range for preparing pseudoboehmite using different sodium aluminate solution concentrations and examines the influence of α_k on the critical end point pH values. The study clarifies the reaction control conditions for preparing pseudoboehmite through the carbonation reaction with different sodium aluminate solution concentrations and α_k. Furthermore, by analyzing pH changes of liquid phase and the evolution of crystalline phases after the carbonation reaction, the new nucleation mechanism of pseudoboehmite and Bayerite crystals and the root cause of effect of the carbonation reaction end point pH on aluminum hydroxide crystalline phases was proposed. Lastly, the study investigates the properties of pseudoboehmite prepared at different carbonation reaction end point pH and successfully synthesizes and characterizes mesoporous activated alumina. This research provides an in-depth exploration of the critical end point pH values and mechanisms essential for the precise control of the carbonation method in producing pseudoboehmite. This not only contributes to the precise control of the reaction process and improves the control level of the production process,

https://doi.org/10.1021/acs.iecr.3c04662
Ind. Eng. Chem. Res. XXXX, XXX, XXX−XXX

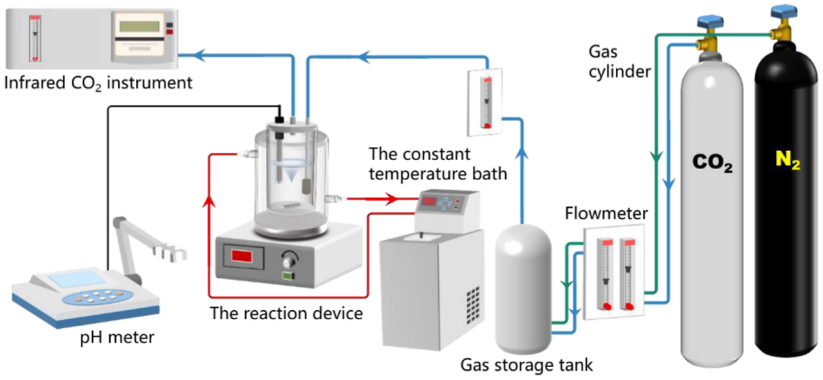

Figure 1. Experimental setup for carbonation reaction.

prevention of impurity generation, and enhancement of production efficiency but also facilitates the efficient utilization of carbon dioxide, avoiding excessive reactions and cost reduction. It amplifies the green and environmentally friendly advantages of the carbonation method in preparing pseudoboehmite.

2. EXPERIMENTAL SECTION

2.1. Material. Analytically pure aluminum hydroxide and sodium hydroxide were purchased from Shanghai McLean Biochemical Technology Co., Ltd. Deionized (DI) water used in all experiments was prepared from an ultrapure water system. The carbon dioxide gas and nitrogen used have a purity of 99.9% and were purchased from Taiyuan Taineng Gas Co., Ltd.

2.2. Procedures. *2.2.1. Preparation of Sodium Aluminate Solution.* Deionized water, solid sodium hydroxide, and aluminum hydroxide were sequentially placed in a high-pressure reactor (purchased from Xi'an Taikang Technology Co., Ltd.) and stirred. The reaction temperature was set at 160 °C, and the reaction time was maintained for 4 h to prepare sodium aluminate solutions with varying concentrations and component ratios (α_k).

2.2.2. Carbonation Reaction between Sodium Aluminate Solution and Carbon Dioxide Gas. The carbonation reaction experimental device and the process for preparing pseudoboehmite and activated alumina are shown in Figures 1 and 2.

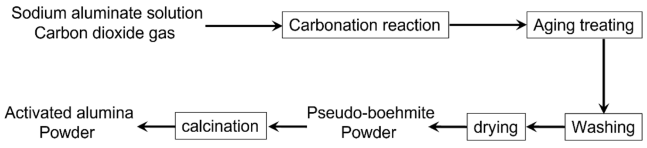

Figure 2. Process flowchart for preparing pseudoboehmite and alumina.

The sodium aluminate solution was placed in a jacketed glass reactor and continuously stirred; its temperature was controlled by a constant temperature water bath, and then 0.8 L/min carbon dioxide gas was continuously introduced. At the same time, a pH meter (INESA PHS-3C) was used to measure and record the pH changes in the liquid during the carbonation reaction in real time. The reacted material liquid was aged and then washed and dried to prepare aged powder. The aging treatment was to heat the material liquid to the aging temperature of 90 °C and keep the temperature constant for 3 h. Pseudoboehmite was calcined at 550 °C for 2.5 h to prepare alumina powder.

2.3. Characterization. To identify the crystal form, powder X-ray diffraction (XRD) patterns were recorded using TTR with Cu KR (45 kV and 200 mA) between 5 and 85° at a scan speed of 10°/min. The N_2 adsorption/desorption isotherms for PB and MA were obtained by a Quantachrome Autosorb-IQ using a static adsorption procedure, and the samples were outgassed at 300 °C vacuums below 10^{-3} Torr for 5 h prior to the measurements. The Brunauer–Emmett–Teller surface area was calculated from the adsorption data in the relative pressure range of 0.05–0.25, the pore diameter was determined by applying the Barrett–Joyner–Halenda (BJH) model to the isotherm adsorption branches, and the total pore volume was determined from the amount adsorbed at a relative pressure of 0.995. The morphologies of particles and the membrane were observed using scanning electron microscopy (SEM, JEM-6301F Japan). Fourier transform infrared spectra were obtained on a PerkinElmer Spectrum Two FT-IR Spectrometer.

3. RESULTS AND DISCUSSION

3.1. Effect of Sodium Aluminate Solution Concentration and Component Ratios (α_k) on Preparation of Pseudoboehmite with Carbonation Reaction. *3.1.1. Effect on pH Change of Sodium Aluminate Solution during Carbonation Reaction.* The pH change curves during the carbonation process of sodium aluminate solutions with different concentrations and component ratios (α_k) are depicted in Figure 3. The curve could be divided into three stages: in the first stage, a rapid decrease in pH occurred until a turning point was reached, at which point a substantial number of solid precipitates was observed; in the second stage, the pH decline rate stabilized, with continuous solid precipitation; in the third stage, the pH decline rate accelerated again until the carbonation reaction ceased and the pH remained constant. The pH values at the turning points of 0.1–0.5 mol/L sodium aluminate solutions (α_k = 2.0) were around 11.04, 11.31, 11.47, 11.59, and 11.71, respectively, as shown in Figure 3A. The corresponding α_k values of these solutions at the turning points were approximately 1.0110, 1.0102, 1.0098, 1.0097, and 1.0102. This indicated that in the first stage, the reaction between carbon dioxide and free sodium hydroxide led to a rapid decrease in pH and α_k. As α_k decreased to approximately 1.01, sodium aluminate became oversaturated, resulting in the decomposition of sodium aluminate to generate precipitates and hydroxide ions. Subsequently, in the second stage, the

https://doi.org/10.1021/acs.iecr.3c04662
Ind. Eng. Chem. Res. XXXX, XXX, XXX–XXX

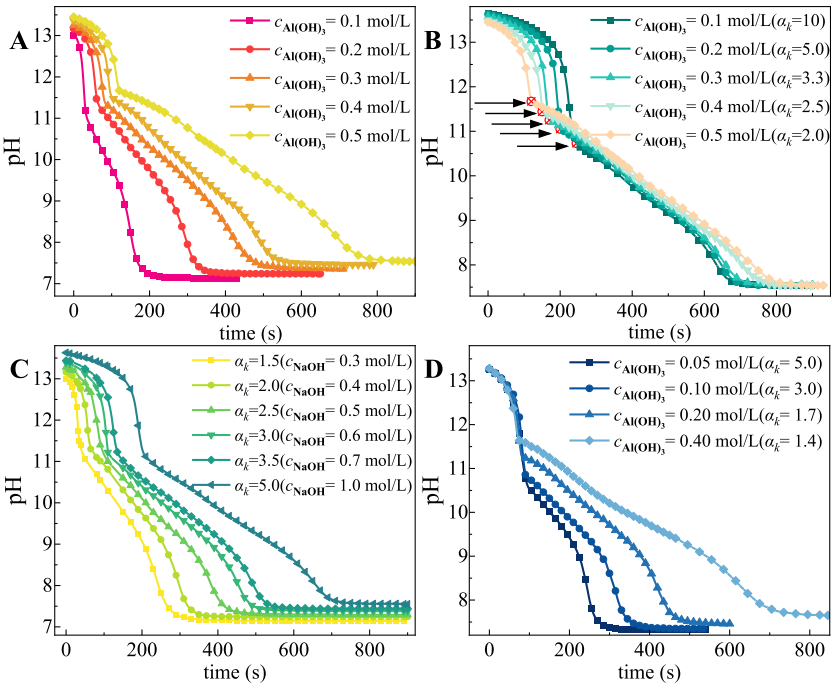

Figure 3. pH change curve during the carbonation reaction of different sodium aluminate solutions. (A) α_k = 2.0. (B) c_{NaOH} = 1.0 mol/L. (C) $c_{Al(OH)_3}$ = 0.2 mol/L. (D) 0.2 mol/L the concentration of free sodium hydroxide was 0.2 mol/L.

lower concentration of hydroxide ions in the solution led to a slower rate of carbonation reaction, causing deceleration in the pH reduction. Finally, in the third stage, with extremely low concentration of sodium aluminate, the bicarbonate ions gradually saturated, and both the carbonation reaction and decomposition of sodium aluminate ceased to occur.

As shown in Figure 3A, the α_k of the sodium aluminate solution remains unchanged at 2.0. With the aluminum hydroxide concentration of the solution increased, that is, the concentration of sodium aluminate increased, the initial pH of the solution, the turning point pH of curve and the final point pH of the reaction increased. As depicted in Figure 3B, the total sodium hydroxide concentration was maintained at 1.0 mol/L. As the aluminum hydroxide concentration of the solution increased and α_k decreased, the initial pH decreased, the turning point pH increased, the pH decreases rate in the second stage, and the final point pH remained unchanged. When the concentration of aluminum hydroxide was 0.2 mol/L, with increasing sodium hydroxide concentration, that is, increasing α_k, the turning point pH weak decreased, the initial pH and final point pH increased, as illustrated in Figure 3C. When the concentration of free sodium hydroxide was 0.2 mol/L, the increase in the concentration of aluminum hydroxide, i.e., the decrease in α_k, resulted in equal initial pH, an increase in the turning point pH, and an increase in the final reaction point pH, as illustrated in Figure 3D.

The research indicated that the concentration of free sodium hydroxide in sodium aluminate solution determined the initial pH of the solution and the reaction time of the first stage. With an increase in the concentration of free sodium hydroxide, the initial pH and reaction time also increased accordingly. The concentration of sodium aluminate in the solution determined the turning point pH and the reaction time of the second stage. As the concentration of sodium aluminate increased, the turning point pH and reaction time also increased. The total concentration of sodium hydroxide in the solution determined the final point pH of the reaction and the reaction rate of the second stage. Therefore, reducing the concentration of free sodium hydroxide, i.e., decreasing the solution's α_k, was beneficial for enhancing the reaction rate of the second stage and shortening the overall reaction time. The concentration and α_k of sodium aluminate solution affected the critical pH and reaction process of the precipitation in the carbonation reaction. Furthermore, the influence on the end point pH of the carbonation reaction for the preparation of pseudoboehmite was investigated.

3.1.2. Effect of Sodium Aluminate Concentration on the Carbonation Reaction End Point pH Critical Value of Preparing Pseudoboehmite. The influence of sodium aluminate solution concentration on the critical end point pH of the carbonation reaction for preparing pseudoboehmite was investigated through experimental studies, and the results are presented in Table 1. XRD analysis revealed the formation of pseudoboehmite (JCPDS·no. 49-0133), bayerite (JCPDS·no. 20-0011), gibbsite (JCPDS·no. 33-0018), and Dawsonite (JCPDS·no. 45-1359) for different concentrations of sodium aluminate solutions, as detailed in Table 1. At the higher end point pH values, the carbonation reaction produced bayerite and gibbsite, as illustrated in Figure 4 and the records for experiments 1−16 in Table 1. Specifically, when the end point pH of the carbonation reaction was less than 10.3, the precipitate obtained from a 0.1 mol/L sodium aluminate solution was identified as pseudoboehmite. Correspondingly, at end point pH values less than 10.6, 10.8, and 11.2, the precipitates from 0.2, 0.3, and 0.5 mol/L sodium aluminate solutions were pseudoboehmite. The study indicated that the maximum end point pH values for the carbonation reaction of pseudoboehmite preparation using 0.1, 0.2, 0.3, and 0.5 mol/L sodium aluminate solutions were 10.3, 10.6, 10.8, and 11.2, respectively. Infrared analysis confirmed the consistency with XRD results, showing absorption peaks of bayerite at 3656, 3550 cm^{-1} and gibbsite at 3620, 3528, 1456, 1036 cm^{-1} in

https://doi.org/10.1021/acs.iecr.3c04662
Ind. Eng. Chem. Res. XXXX, XXX, XXX−XXX

Table 1. Experimental Results Table of the Effect of Sodium Aluminate Concentration on the End Point of the Carbonation Reaction for the Preparation of Pseudoboehmite[a]

numbers	c_{NaAlO_2}/(mol/L)	α_k	pH_R	crystalline phase
1	0.1	2	10.5	B
2	0.1	2	10.4	B
3	0.1	2	10.3	PB
4	0.1	2	10.0	PB
5	0.2	2	10.7	B + G
6	0.2	2	10.6	PB
7	0.2	2	10.5	PB
8	0.2	2	10.4	PB
9	0.3	2	11.0	B + G
10	0.3	2	10.9	B
11	0.3	2	10.8	PB
12	0.3	2	10.7	PB
13	0.5	2	11.4	B + G
14	0.5	2	11.3	B
15	0.5	2	11.2	PB
16	0.5	2	11.1	PB
17	0.1	2	8.2	PB
18	0.1	2	8.0	DA
19	0.2	2	8.5	PB
20	0.2	2	8.3	DA
21	0.3	2	9.0	PB
22	0.3	2	8.7	DA
23	0.5	2	9.5	PB
24	0.5	2	9.3	DA
25	0.2	1.5	11.0	B
26	0.2	1.5	10.8	PB
27	0.2	2.5	10.6	B
28	0.2	2.5	10.4	PB
29	0.2	1.5	8.2	PB
30	0.2	1.5	8.0	DA
31	0.2	2.5	8.7	PB
32	0.2	2.5	8.5	DA

[a]Reaction temperature T_R = 25 °C, the end point pH_R, aging temperature T_A = 90 °C, aging time t_A = 3 h, drying temperature T_D = 80 °C, drying time t_D = 6 h; PB: pseudoboehmite, B: bayerite, G: gibbsite, DA: Dawsonite.

Figure 5. At lower end point pH values, the precipitate formed in the carbonation reaction was identified as Dawsonite, as detailed in Figure 6 and the records for experiments 17−24 in Table 1. At the end point pH ≤ 8.0, the precipitate obtained from a 0.1 mol/L sodium aluminate solution was Dawsonite, while at end point pH values ≤ 8.7, 9.0, and 9.5, the precipitates from 0.2 0.3, and 0.5 mol/L sodium aluminate solutions were identified as Dawsonite. Somayeh et al.[46] reported that a large amount of sodium bicarbonate (pH less than 10) led to the formation of Dawsonite. The study found that the minimum end point pH values for the carbonation reaction of pseudoboehmite preparation using 0.1, 0.2, 0.3, and 0.5 mol/L sodium aluminate solutions were 8.2, 8.5, 9.0, and 9.5, respectively. In summary, the experimental results indicate that with an increase in sodium aluminate solution concentration, both the maximum and minimum end point pH values for the carbonation reaction in preparing pseudoboehmite exhibit an upward trend. Figure 7 illustrates the critical values curve and range of the reaction end point pH for the carbonation reaction in preparing pseudoboehmite at different concentrations of sodium aluminate solutions, demonstrating a gradual reduction in pH range with increasing concentration. These findings provide an explanation for the previously reported differences in the reaction end point pH values. Therefore, the preparation of pseudoboehmite using the carbonation method not only requires precise control of the end point pH but also demands meticulous adjustment of the concentration of sodium aluminate solution to prevent impurity formation.

3.1.3. Effect of α_k of Sodium Aluminate Solution on the Carbonation Reaction End Point pH Critical Value of Preparing Pseudoboehmite. The influence of α_k in sodium aluminate solutions on the critical end point pH of the carbonation reaction for preparing pseudoboehmite was investigated, and the specific experimental results are presented in Table 1, experiments 25−32. The XRD patterns of the precipitates corresponding to different α_k values are illustrated in Figure 8. At α_k = 2.5, bayerite was formed in the reaction end point pH = 10.6, while at α_k = 1.5, pseudoboehmite was still generated in the reaction end point pH = 10.8. At α_k = 2.5, Dawsonite was produced in the reaction end point pH = 8.5, and at α_k = 1.5, pseudoboehmite was formed in the reaction end point pH = 8.2. Experiment indicated that the maximum values of the carbonation reaction end point pH for preparing pseudoboehmite with α_k values of 1.5, 2.0, and 2.5 are 10.8, 10.6, and 10.4, respectively, while the corresponding minimum values are 8.2, 8.5, and 8.7. The maximum end point pH for preparing pseudoboehmite decreased with increasing α_k, while the minimum end point pH increased with α_k. The results demonstrated that the generation of sodium carbonate and bicarbonate during the carbonation reaction inhibits the decomposition reaction of sodium aluminate, thereby reducing the maximum end point pH for pseudoboehmite formation. This was reflected in the pH change curve of the carbonation reaction, where the turning point pH decreased with increasing α_k. Sodium carbonate and bicarbonate facilitated the crystal growth of Dawsonite, increased the maximum end point pH for the carbonation reaction to produce Dawsonite, and raised the minimum end point pH for pseudoboehmite formation. This finding aligned with results from Marinos et al.,[21] who reported that increasing the initial concentration of sodium carbonate in sodium aluminate solutions promoted the formation of Dawsonite. Furthermore, the critical curve and range of the reaction end point pH for preparing pseudoboehmite with different α_k values are plotted in Figure 9. As α_k increases, the pH range for the carbonation reaction end point to produce pseudoboehmite gradually narrowed, indicating that an increase in α_k was unfavorable for pseudoboehmite preparation. This study elucidated the impact of sodium aluminate solution on the end point pH of the carbonation reaction for preparing pseudoboehmite. This not only facilitated precise control of the reaction process, enhancing production efficiency, but also contributed to the efficient utilization of carbon dioxide, preventing overreaction and improving reactant utilization. Bayerite and Dawsonite are widely used powders, making this research highly relevant for the carbonation method in the preparation of bayerite and Dawsonite.

3.2. Nucleation Mechanism of Pseudoboehmite and Bayerite Crystals and the Root Cause of Effect of the Carbonation Reaction End Point pH on the Nucleation. The study investigated the crystalline structure of the solid generated by the carbonation reaction before aging treatment,

https://doi.org/10.1021/acs.iecr.3c04662
Ind. Eng. Chem. Res. XXXX, XXX, XXX−XXX

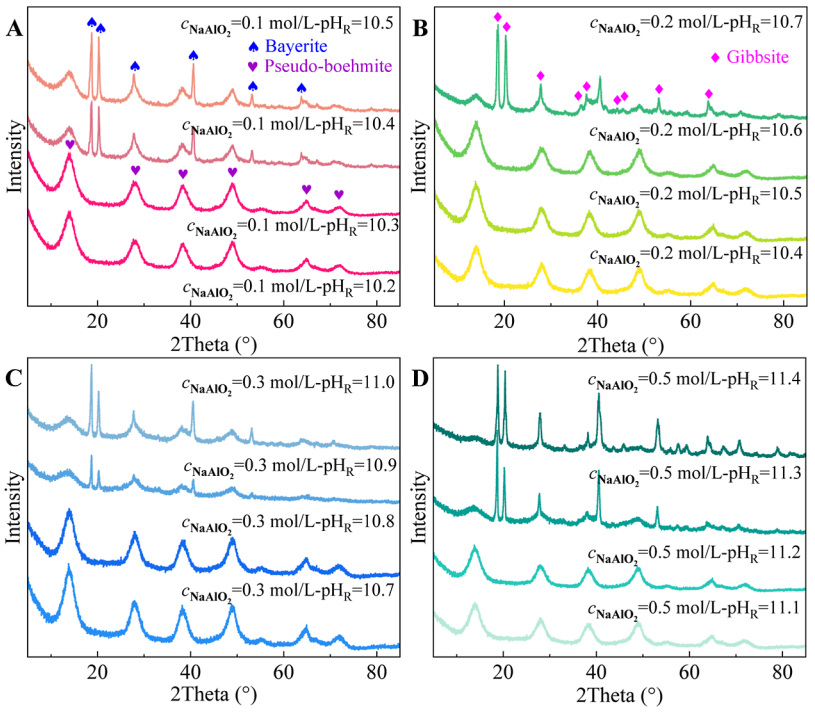

Figure 4. XRD patterns of precipitates produced by carbonation reaction with different concentrations of sodium aluminate solution [(A) c_{NaAlO_2} = 0.1 mol/L; (B) c_{NaAlO_2} = 0.2 mol/L; (C) c_{NaAlO_2} = 0.3 mol/L; (D) c_{NaAlO_2} = 0.4 mol/L; α_k = 2.0].

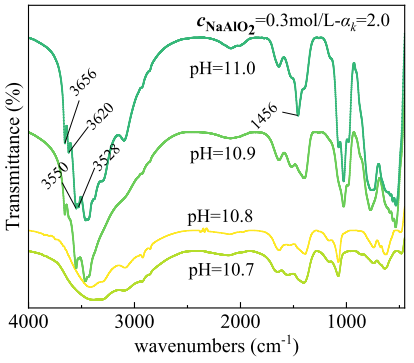

Figure 5. Infrared spectra of precipitates produced by carbonation reaction at 0.3 mol/L sodium aluminate solution.

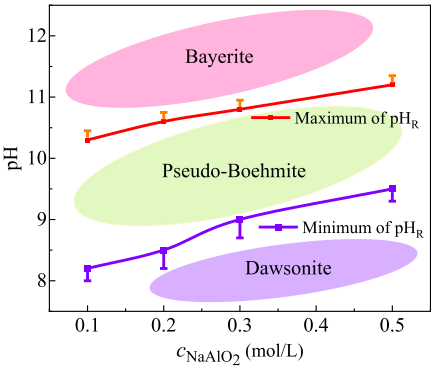

Figure 7. Critical values curve and range of the reaction end point pH for the carbonation reaction in preparing pseudoboehmite at different concentrations of sodium aluminate solutions (α_k = 2.0).

with XRD spectra presented in Figure 10. None of the solid samples before aging exhibited characteristic peaks of any crystals. This indicated that the solid formed through the carbonation reaction was amorphous aluminum hydroxide. Under suitable carbonation reaction end point pH, pseudo-

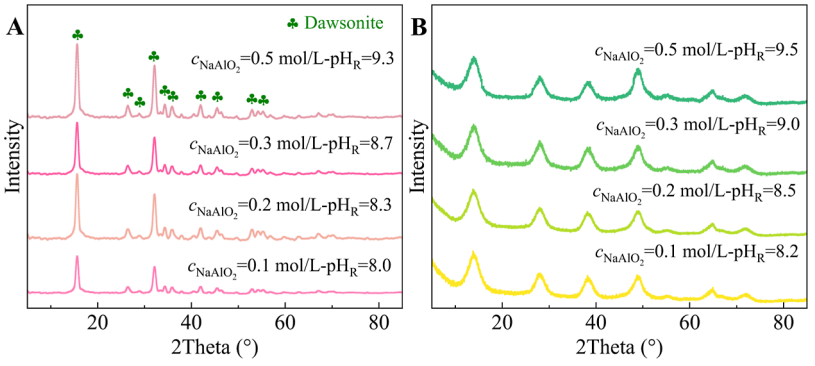

Figure 6. XRD patterns of precipitates produced by carbonation reaction with different concentrations of sodium aluminate solution (α_k = 2.0).

https://doi.org/10.1021/acs.iecr.3c04662
Ind. Eng. Chem. Res. XXXX, XXX, XXX−XXX

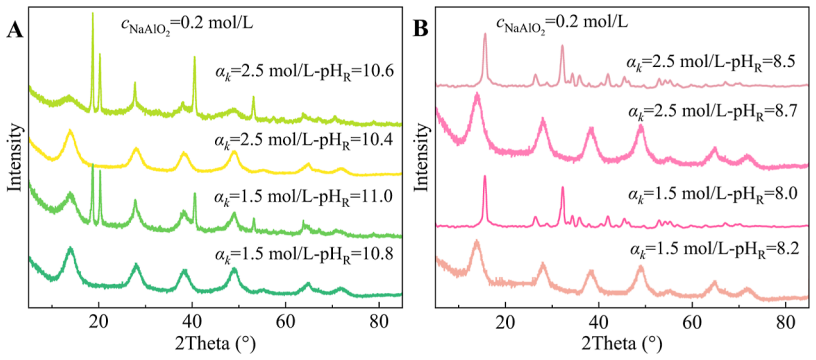

Figure 8. XRD patterns of precipitates produced by carbonation reaction with different α_k values of sodium aluminate solution.

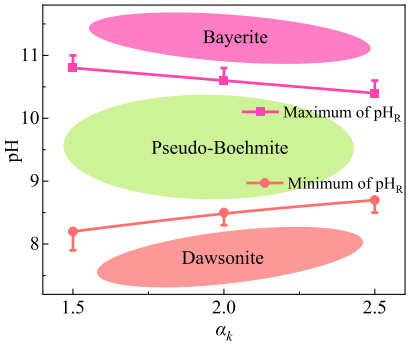

Figure 9. Critical values curve and range of the reaction end point pH for the carbonation reaction in preparing pseudoboehmite at different α_k of 0.2 mol/L sodium aluminate solutions.

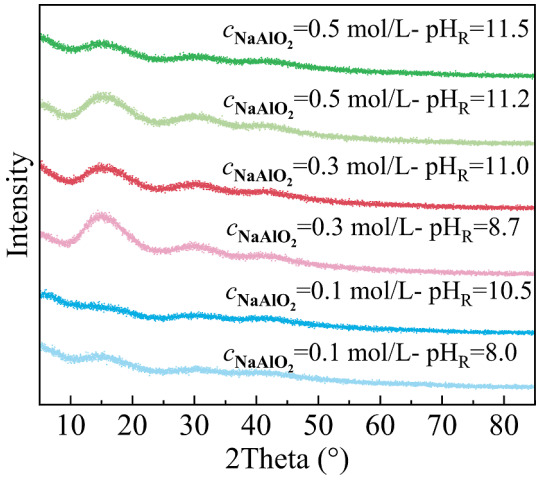

Figure 10. XRD pattern of the solid generated by the carbonation reaction before aging treatment.

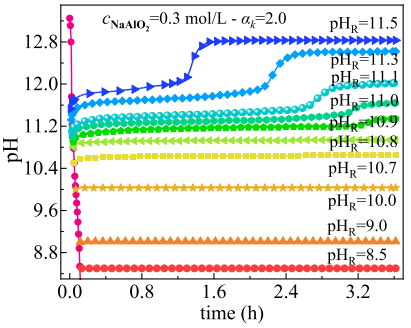

Figure 11. PH change of aluminum sodium solution after the carbonation reaction during settling. pH$_R$: the end point pH of sodium aluminate solution;.

boehmite was generated by amorphous aluminum hydroxide during the aging process. Conversely, at higher and lower carbonation reaction end point pH, bayerite and Dawsonite crystals were formed, respectively.

To explore the reasons behind these phenomena, the pH change of aluminum sodium solution and crystalline phase evolution after the carbonation reaction during settling were examined, as shown in the pH change curve in Figure 11. The steep curve on the far left was the pH curve of the carbonation reaction. After the carbonation reaction, the pH of the sodium aluminate solution increased significantly, indicating that the solution continued to decompose into the precipitation of aluminum hydroxide and hydroxyl ions, which led to the increase of pH value. When the carbonation reaction end point pH exceeded 10, the pH curve exhibited a rapid increase immediately after the carbonation reaction ceased. For carbonation reaction end point pH values ranging from 10.9 to 11.5, after a period of settling, the pH experienced a second significant increase. However, at pH values of 10.8, 10.7, and 10, the pH curve showed only one increase without a second significant rise. At pH values of 9.0 and 8.5, there was no pronounced change in the pH curve. XRD analysis of the precipitation during settling, as depicted in Figure 12, revealed that at the carbonation reaction end point pH of 11.5, the solid formed after 0.2 h of settling did not exhibit any characteristic peaks. In contrast, the solid formed after 1.5 h settling displayed characteristic peaks of bayerite crystals. At the carbonation reaction end point pH of 11.0, the solid formed after 0.5 h settling did not show characteristic peaks, while the solid formed after 3.5 h settling exhibited characteristic peaks of bayerite crystal. When the carbonation reaction end point pH was 10.8, the solid formed after 3.5 h settling did not show any characteristic peaks. Lastly, at the carbonation reaction end point pH of 8.5, the solid formed after 3.5 h settling displayed characteristic peaks of Dawsonite.

The experimental results indicated the formation of the bayerite nucleus during the second decomposition reaction. Bayerite and pseudoboehmite nuclei were generated through different decomposition reactions of sodium aluminate, with the second decomposition reaction being the fundamental cause for the formation of the bayerite nucleus. Contrary to the long-standing belief that bayerite grows from amorphous aluminum hydroxide and pseudoboehmite,[7] this study challenged the crystal growth mechanism, suggesting that the bayerite nucleus is not formed by the growth of amorphous

https://doi.org/10.1021/acs.iecr.3c04662
Ind. Eng. Chem. Res. XXXX, XXX, XXX−XXX

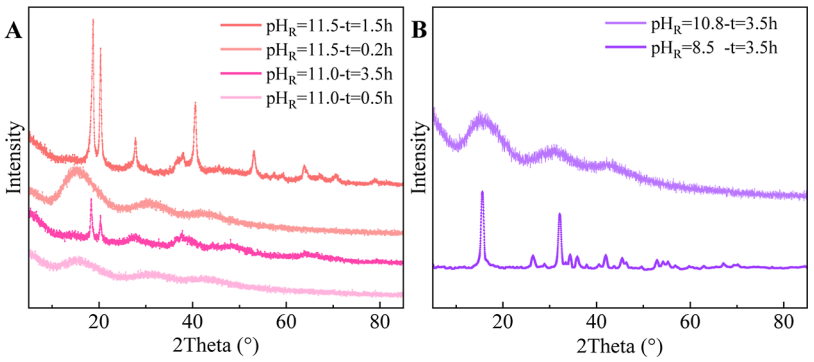

Figure 12. XRD pattern of precipitation during settling.

aluminum hydroxide and pseudoboehmite. Reducing the end point pH of the carbonation reaction accelerated the decomposition reaction to produce pseudoboehmite and inhibited the decomposition reaction to form bayerite. When the end point pH of the carbonation reaction was relatively high, the aging process provided time for the second decomposition reaction of the sodium aluminate solution, leading to the formation of bayerite crystals. This explanation clarified the impact of the carbonation reaction end point on crystal phases and the mechanism of aluminum hydroxide crystal growth. Additionally, the two forms of aluminate ions need to be further studied to investigate the reasons for the two different decomposition processes in the sodium aluminate solutions. Accurate control of the carbonation reaction end point pH is essential for the preparation of pseudoboehmite. This is not only to prevent the second decomposition reaction of aluminum sodium during aging, resulting in the impurity of bayerite, but also to prevent the growth of amorphous aluminum hydroxide into Dawsonite crystals.

3.3. Textural Properties of Pseudoboehmite and Activated Alumina Prepared by the Carbonation Reaction. In the investigation of sodium aluminate solutions with concentrations of 0.1, 0.2, 0.3, and 0.5 mol/L, the carbonation reaction end point pH for the preparation of pseudoboehmite in a 0.4 mol/L sodium aluminate solution (α_k = 2.0) was predicted to reach a maximum value of 11.0. The resulting precipitate was analyzed, and the XRD spectrum, presented in Figure 13, displayed characteristic peaks of pseudoboehmite. This confirmation reinforced the accuracy of the critical curve for the carbonation reaction end point pH during pseudoboehmite preparation. Subsequently, the prepared pseudoboehmite underwent calcination at 550 °C for 2.5 h to yield alumina, a transformation verified through crystalline phase analysis, as depicted in Figure 13. Notably, the characteristic peaks of the sample closely matched those of activated alumina (JCPDS·no. 49-0134). The structural properties of the prepared pseudoboehmite and activated alumina were investigated. Figure 14A depicts the N_2 adsorption−desorption isotherms for both samples, providing measurements of the specific surface area and pore volume. Pore size distribution, determined using the BJH method, was illustrated in Figure 14B, with a summary of textural features in Table 2. Clear from Figure 14A is the classic Type IV shape with hysteresis loops in all isotherms, signifying the mesoporous nature of the materials. Both pseudoboehmite and alumina samples exhibited H2-type hysteresis loops, indicating ink-bottle-shaped pores. Interestingly, the hysteresis loop of activated alumina shifted to a region of relatively higher pressure compared to that of pseudoboehmite, indicating an increase in mesopore size, as evident in the PSD curve in Figure 14. Pore volumes for pseudoboehmite and activated alumina were measured at 0.41 and 0.44 cm^3/g, with specific surface areas of 440.72 and 242.76 m^2/g, and average pore diameters of 3.7 and 7.3 nm, respectively. The structural properties of pseudo¯boehmite and activated alumina prepared using this method aligned with those obtained through alternative approaches. SEM revealed a block-like structure for pseudoboehmite and a porous structure for activated alumina, as shown in Figure 15.

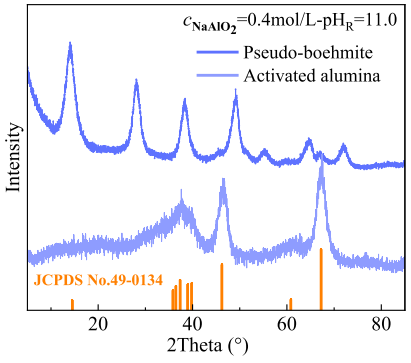

Figure 13. XRD pattern of pseudoboehmite and activated alumina.

4. CONCLUSIONS

The reaction end point pH served as the most critical control parameter in the carbonation reaction for the preparation of pseudoboehmite. This study investigated the influence of sodium aluminate solution concentration and composition ratio (α_k) on pH change during the carbonation reaction, examining the impact of concentration and α_k on the reaction end point pH critical values of pseudoboehmite preparation. Further, the fundamental reasons for the influence of carbonation reaction end point pH on crystal structure were explored, along with the growth mechanisms of pseudoboehmite and bayerite crystals during the preparation process. The research revealed that concentration and α_k significantly affected the pH change during the carbonation reaction. The end point pH range and influence pattern of sodium aluminate solutions with different component structures on the carbonation reaction for pseudoboehmite preparation were clarified and explained, avoiding overreaction. Notably, with the increase in concentration, both the maximum and minimum values of the end point pH for pseudoboehmite

https://doi.org/10.1021/acs.iecr.3c04662
Ind. Eng. Chem. Res. XXXX, XXX, XXX−XXX

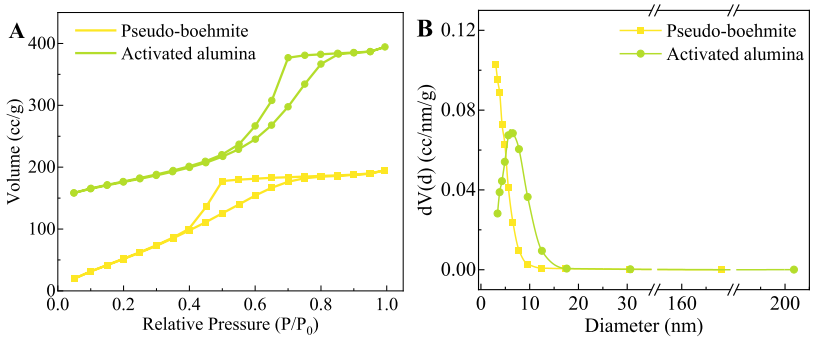

Figure 14. N_2 adsorption−desorption isotherms and BJH pore size distribution for pseudoboehmite and activated alumina prepared the carbonation reaction.

Table 2. Textual Properties of Pseudoboehmite and Activated Alumina

sample	surface area/(m^2/g)	pore volume/(m^3/g)	pore diameter/nm
pseudoboehmite	440.72	0.41	3.7
activated alumina	242.76	0.44	7.3

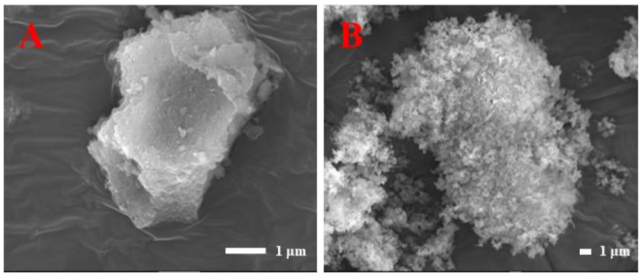

Figure 15. SEM images of pseudoboehmite (A) and activated alumina (B).

preparation increased. As α_k increased, the maximum value of the end point pH for preparing pseudoboehmite decreased, while the minimum value increased. More importantly, increasing concentration and α_k both narrowed the end point pH range for pseudoboehmite preparation. A groundbreaking revelation challenges the conventional understanding of the crystal growth mechanism of aluminum hydroxide. Nucleation of pseudoboehmite and bayerite crystals originated from two distinct pathways of sodium aluminate decomposition. By reducing the carbonation reaction end point pH, the decomposition reaction for preparation of pseudoboehmite was accelerated, simultaneously suppressing the decomposition reaction for bayerite. Ultimately, under the predicted carbonation reaction end point pH, mesoporous pseudoboehmite and active alumina were successfully prepared, with the pore volume of 0.44 cm^3/g, the specific surface area of 242.76 m^2/g, and the average pore diameter of 7.3 nm. This study not only addressed the challenge of impurity formation in the carbonation reaction, leading to bayerite, but also achieved precise control of crystal nucleation, enhancing production efficiency. Additionally, it facilitated the efficient utilization of carbon dioxide and promoted a more environmentally friendly and economically viable production process.

■ ASSOCIATED CONTENT

Data Availability Statement

All data could be found in the experimental part.

■ AUTHOR INFORMATION

Corresponding Author

Youzhi Liu − *School of Chemistry and Chemical Engineer, North University of China, Taiyuan 030051, PR China; Shanxi Province Key Laboratory of Higee-Oriented Chemical Engineering, Taiyuan 030051, PR China*; Email: liuyz@nuc.edu.cn

Authors

Chengqian Zhang − *School of Chemistry and Chemical Engineer, North University of China, Taiyuan 030051, PR China; Shanxi Province Key Laboratory of Higee-Oriented Chemical Engineering, Taiyuan 030051, PR China;* orcid.org/0009-0005-1103-6409

Yuliang Li − *School of Chemistry and Chemical Engineer, North University of China, Taiyuan 030051, PR China; Shanxi Province Key Laboratory of Higee-Oriented Chemical Engineering, Taiyuan 030051, PR China*

Shuwei Guo − *School of Chemistry and Chemical Engineer, North University of China, Taiyuan 030051, PR China; Shanxi Province Key Laboratory of Higee-Oriented Chemical Engineering, Taiyuan 030051, PR China*

Shufei Wang − *School of Chemistry and Chemical Engineer, North University of China, Taiyuan 030051, PR China; Shanxi Province Key Laboratory of Higee-Oriented Chemical Engineering, Taiyuan 030051, PR China*

Shangyuan Cheng − *School of Chemistry and Chemical Engineer, North University of China, Taiyuan 030051, PR China; Shanxi Province Key Laboratory of Higee-Oriented Chemical Engineering, Taiyuan 030051, PR China*

Hongyan Shen − *School of Chemistry and Chemical Engineer, North University of China, Taiyuan 030051, PR China; Shanxi Province Key Laboratory of Higee-Oriented Chemical Engineering, Taiyuan 030051, PR China*

Complete contact information is available at: https://pubs.acs.org/10.1021/acs.iecr.3c04662

Notes

The authors declare no competing financial interest.

■ ACKNOWLEDGMENTS

Thanks for the funding support of this research from National Natural Science Foundation of China (General Program, 22378370), National Natural Science Foundation of China (22108261, 22108263), the Natural Science Foundation of Shanxi Province (20210302124060), and the Graduate Research Project of North University of China (20221826).

https://doi.org/10.1021/acs.iecr.3c04662
Ind. Eng. Chem. Res. XXXX, XXX, XXX−XXX

REFERENCES

(1) Al-Khattaf, S. The influence of alumina on the performance of FCC catalysts during hydrotreated VGO catalytic cracking. *Energy Fuels* **2003**, *17*, 62−68.

(2) Tian, K.; Li, Q.; Jiang, W.; Wang, X.; Liu, S.; Zhao, Y.; Zhou, G. Effect of the pore structure of an active alumina catalyst on isobutene production by dehydration of isobutanol. *RSC Adv.* **2021**, *11*, 11952−11958.

(3) Liu, Y.; Qing, S.; Hou, X.; Qin, F.; Wang, X.; Gao, Z.; Xiang, H. Temperature dependence of Cu−Al spinel formation and its catalytic performance in methanol steam reforming. *Catal. Sci. Technol.* **2017**, *7*, 5069−5078.

(4) Keyvanloo, K.; Mardkhe, M. K.; Alam, T. M.; Bartholomew, C. H.; Woodfield, B. F.; Hecker, W. C. Supported Iron Fischer−Tropsch Catalyst: Superior Activity and Stability Using a Thermally Stable Silica-Doped Alumina Support. *ACS Catal.* **2014**, *4*, 1071−1077.

(5) Liu, C.; Li, J.; Liew, K.; Zhu, J.; Nordin, M. R. b. An environmentally friendly method for the synthesis of nano-alumina with controllable morphologies. *RSC Adv.* **2012**, *2*, 8352−8358.

(6) Majhi, A.; Pugazhenthi, G.; Shukla, A. Comparative Study of Ultrasound Stimulation and Conventional Heating Methods on the Preparation of Nanosized γ-Al2O3. *Ind. Eng. Chem. Res.* **2010**, *49*, 4710−4719.

(7) Zhang, H.; Zhang, X.; Graham, T. R.; Pearce, C. I.; Hlushko, H.; LaVerne, J. A.; Liu, L.; Wang, S.; Zheng, S.; Zhang, Y.; Clark, S. B.; Li, P.; Wang, Z.; Rosso, K. M. Crystallization and Phase Transformations of Aluminum (Oxy)hydroxide Polymorphs in Caustic Aqueous Solution. *Inorg. Chem.* **2021**, *60*, 9820−9832.

(8) Du, X.; Wang, Y.; Su, X.; Li, J. Influences of pH value on the microstructure and phase transformation of aluminum hydroxide. *Powder Technol.* **2009**, *192*, 40−46.

(9) Kocjan, A.; Dakskobler, A.; Kosmač, T. Evolution of Aluminum Hydroxides in Diluted Aqueous Aluminum Nitride Powder Suspensions. *Cryst. Growth Des.* **2012**, *12*, 1299−1307.

(10) Lefèvre, G.; Pichot, V.; Fédoroff, M. Controlling Particle Morphology during Growth of Bayerite in Aluminate Solutions. *Chem. Mater.* **2003**, *15*, 2584−2592.

(11) Li, Y.; Zhang, Y.; Chen, F.; Yang, C.; Zhang, Y. Polymorphic Transformation of Aluminum Hydroxide Precipitated from Reactive NaAl(OH)4−NaHCO3 Solution. *Cryst. Growth Des.* **2011**, *11*, 1208−1214.

(12) Zhang, X.; Cui, W.; Hu, J. Z.; Wang, H.-W.; Prange, M. P.; Wan, C.; Jaegers, N. R.; Zong, M.; Zhang, H.; Pearce, C. I.; Li, P.; Wang, Z.; Clark, S. B.; Rosso, K. M. Transformation of Gibbsite to Boehmite in Caustic Aqueous Solution at Hydrothermal Conditions. *Cryst. Growth Des.* **2019**, *19*, 5557−5567.

(13) Zhang, X.; Cui, W.; Page, K. L.; Pearce, C. I.; Bowden, M. E.; Graham, T. R.; Shen, Z.; Li, P.; Wang, Z.; Kerisit, S.; N'Diaye, A. T.; Clark, S. B.; Rosso, K. M. Size and Morphology Controlled Synthesis of Boehmite Nanoplates and Crystal Growth Mechanisms. *Cryst. Growth Des.* **2018**, *18*, 3596−3606.

(14) Balakrishnan, K.; Gonzalez, R. D. Preparation of Bimetallic Pt-Sn/Alumina Catalysts by the Sol-Gel Method. *Langmuir* **1994**, *10*, 2487−2490.

(15) Fulvio, P. F.; Brosey, R. I.; Jaroniec, M. Synthesis of Mesoporous Alumina from Boehmite in the Presence of Triblock Copolymer. *ACS Appl. Mater. Interfaces* **2010**, *2*, 588−593.

(16) Wang, Z.-M.; Lin, Y. S. Sol−Gel-Derived Alumina-Supported Copper Oxide Sorbent for Flue Gas Desulfurization. *Ind. Eng. Chem. Res.* **1998**, *37*, 4675−4681.

(17) Chen, Y.; Feng, Q. M.; Shao, Y. H.; Zhang, G. F.; Ou, L. M.; Lu, Y. P. Research on the recycling of valuable metals in spent Al2O3-based catalyst. *Miner. Eng.* **2006**, *19*, 94−97.

(18) Asadi, A. A.; Alavi, S. M.; Royaee, S. J.; Bazmi, M. Ultra-deep Hydrodesulfurization of Feedstock Containing Cracked Gasoil through NiMo/γ-Al2O3 Catalyst Pore Size Optimization. *Energy Fuels* **2018**, *32*, 2203−2212.

(19) Handjani, S.; Blanchard, J.; Marceau, E.; Beaunier, P.; Che, M. From mesoporous alumina to Pt/Al2O3 catalyst: A comparative study of the aluminas synthesis in aqueous medium, physicochemical properties and stability. *Microporous Mesoporous Mater.* **2008**, *116*, 14−21.

(20) Jiang, Y.-F.; Liu, C.-L.; Xue, J.; Li, P.; Yu, J.-G. Insights into the polymorphic transformation mechanism of aluminum hydroxide during carbonation of potassium aluminate solution. *CrystEngComm* **2018**, *20*, 1431−1442.

(21) Marinos, D.; Kotsanis, D.; Alexandri, A.; Balomenos, E.; Panias, D. Carbonation of Sodium Aluminate/Sodium Carbonate Solutions for Precipitation of Alumina Hydrates-Avoiding Dawsonite Formation. *Crystals* **2021**, *11* (7), 836.

(22) Shayanfar, S.; Aghazadeh, V.; Saravari, A.; Hasanpour, P. Aluminum hydroxide crystallization from aluminate solution using carbon dioxide gas: Effect of temperature and time. *J. Cryst. Growth* **2018**, *496−497*, 1−9.

(23) Wang, D.-G.; Guo, F.; Chen, J.-F.; Liu, H.; Zhang, Z.-T. Preparation of nano aluminium trihydroxide by high gravity reactive precipitation. *Chem. Eng. J.* **2006**, *121*, 109−114.

(24) Yang, Q.; Li, D.; Zhuang, F.; Shi, Y.; Kang, X.; Jin, Z. Studies on conversion mechanism in preparation of pseudo boehmite through neutralization of NaAlO2 solution by CO2. *Chin. J. Catal.* **1997**, *18*, 478−482.

(25) Zhong, L.; Zhang, Y.; Zhang, Y. Cleaner synthesis of mesoporous alumina from sodium aluminate solution. *Green Chem.* **2011**, *13*, 2525−2530.

(26) Lu, G.; Zhang, T.; Feng, W.; Zhang, W.; Wang, Y.; Zhang, Z.; Wang, L.; Liu, Y.; Dou, Z. Preparation and Properties of Pseudo-boehmite Obtained from High-Alumina Fly Ash by a Sintering−CO2 Decomposition Process. *Jom* **2019**, *71*, 499−507.

(27) Mwase, J. M.; Vafeias, M.; Marinos, D.; Dimitrios, P.; Safarian, J. Investigating Aluminum Tri-Hydroxide Production from Sodium Aluminate Solutions in the Pedersen Process. *Processes* **2022**, *10*, 1370.

(28) Blissett, R. S.; Rowson, N. A. A review of the multi-component utilisation of coal fly ash. *Fuel* **2012**, *97*, 1−23.

(29) Matjie, R. H.; Bunt, J. R.; van Heerden, J. H. P. Extraction of alumina from coal fly ash generated from a selected low rank bituminous South African coal. *Miner. Eng.* **2005**, *18*, 299−310.

(30) Wu, Y.; Xu, P.; Chen, J.; Li, L.; Li, M. Effect of Temperature on Phase and Alumina Extraction Efficiency of the Product from Sintering Coal Fly Ash with Ammonium Sulfate. *Chin. J. Chem. Eng.* **2014**, *22*, 1363−1367.

(31) Yan, K.; Zhang, J.; Liu, D.; Meng, X.; Guo, Y.; Cheng, F. Feasible synthesis of magnetic zeolite from red mud and coal gangue: Preparation, transformation and application. *Powder Technol.* **2023**, *423*, 118495.

(32) Xie, M.; Liu, F.; Shi, L.; Zhao, H. Green synthesis of aluminum hydroxide from alumina−silica based solid hazardous waste. *Environ. Technol. Innovation* **2023**, *30*, 103127.

(33) Chen, Y.; Feng, Q.; Zhang, G.; Ou, L.; Lu, Y. Study on the recycling of valuable metals in spent Al2O3-based catalyst. *Miner. Metall. Process.* **2007**, *24*, 30−34.

(34) Matveyeva, A. N.; Pakhomov, N. A.; Murzin, D. Y. Recycling of Wastes from the Production of Alumina-Based Catalyst Carriers. *Ind. Eng. Chem. Res.* **2016**, *55*, 9101−9108.

(35) Peterson, R. A.; Buck, E. C. C.; Chun, J.; Daniel, R. C.; Herting, D. L.; Ilton, E. S.; Lumetta, G. J.; Clark, S. B. Review of the Scientific Understanding of Radioactive Waste at the U.S. DOE Hanford Site. *Environ. Sci. Technol.* **2018**, *52*, 381−396.

(36) Yang, Y.; Xu, Y.; Han, B.; Xu, B.; Liu, X.; Yan, Z. Effects of synthetic conditions on the textural structure of pseudo-boehmite. *J. Colloid Interface Sci.* **2016**, *469*, 1−7.

(37) Graham, T. R.; Dembowski, M.; Hu, J. Z.; Jaegers, N. R.; Zhang, X.; Clark, S. B.; Pearce, C. I.; Rosso, K. M. Intermediate Species in the Crystallization of Sodium Aluminate Hydroxy Hydrates. *J. Phys. Chem. C* **2020**, *124*, 12337−12345.

(38) Nienhuis, E. T.; Pouvreau, M.; Graham, T. R.; Prange, M. P.; Page, K.; Loring, J. S.; Stack, A. G.; Clark, A. E.; Schenter, G. K.; Rosso, K. M.; Pearce, C. I.; Wang, H.-W. Structure and reactivity of

https://doi.org/10.1021/acs.iecr.3c04662
Ind. Eng. Chem. Res. XXXX, XXX, XXX−XXX

sodium aluminate complexes in alkaline solutions. *J. Mol. Liq.* **2022**, *367*, 120379.
(39) Chen, J.-F.; Shao, L.; Guo, F.; Wang, X.-M. Synthesis of nanofibers of aluminum hydroxide in novel rotating packed bed reactor. *Chem. Eng. Sci.* **2003**, *58*, 569−575.
(40) Czajkowski, A.; Noworyta, A.; Krótki, M. Studies and modelling of the process of decomposition of aluminate solutions by carbonation. *Hydrometallurgy* **1981**, *7*, 253−261.
(41) Xiaobin, L.; Nan, L.; Qiusheng, Z.; Tiangui, Q.; Guihua, L.; Zhihong, P. Dawsonite preparation by deep carbonation decomposition of spent liquor from carbonation of sodium aluminate solutions. *J. Cent. S. Univ.* **2016**, *47*, 20−25.
(42) Marinos, D.; Vafeias, M.; Sparis, D.; Kotsanis, D.; Balomenos, E.; Panias, D. Parameters Affecting the Precipitation of Al Phases from Aluminate Solutions of the Pedersen Process: The Effect of Carbonate Content. *Journal of Sustainable Metallurgy* **2021**, *7*, 874−882.
(43) Ren, X.; Liu, Y.; Miao, L. Continuous Carbonation for Synthesis of Pseudo-Boehmite by using Cross-Flow Rotating Packed Bed through the Reaction of NaAlO(2) Solution with CO(2) Gas. *Nanomaterials (Basel)* **2020**, *10*, 263.
(44) Wang, Y.; Xu, D.; Sun, H.; Luo, G. Preparation of Pseudoboehmite with a Large Pore Volume and a Large Pore Size by Using a Membrane-Dispersion Microstructured Reactor through the Reaction of CO2 and a NaAlO2 Solution. *Ind. Eng. Chem. Res.* **2011**, *50*, 3889−3894.
(45) Yang, Q. H.; Liu, B.; Li, D. D.; Shi, Y. H.; Nie, H.; Kang, X. H. Preparation of pseudo-boehmite and γ-Al2O3 support by neutralization of NaAlO2 solution with CO2. *China Petroleum Process. Petrochem. Technol.* **2003**, *1*, 47−51.
(46) Somayeh, S.; Valeh, A.; Abdoullah, S. B. Thermodynamic Modeling and Experimental Studies of Bayerite Precipitation from Aluminate Solution Temperature and pH Effect. *Iran. J. Chem. Chem. Eng.* **2019**, *38*, 229.

https://doi.org/10.1021/acs.iecr.3c04662
Ind. Eng. Chem. Res. XXXX, XXX, XXX−XXX